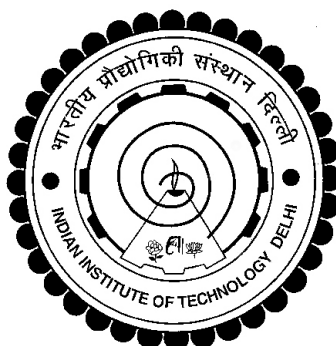


**CARBON FIBER PAPER ELECTRODE OF HIGH
CAPACITANCE FOR SUPERCAPACITOR**

PEPARTHI MYTHILI



**DEPARTMENT OF CHEMICAL ENGINEERING
INDIAN INSTITUTE OF TECHNOLOGY DELHI**

FEBRUARY, 2026

© **Indian Institute of Technology Delhi (IITD), New Delhi, 2026**

Carbon fiber paper electrode of high capacitance for supercapacitor

by

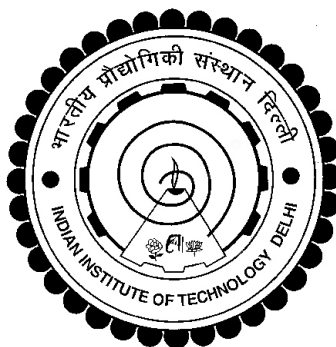
Peparthi Mythili

Department of Chemical Engineering

Submitted

in fulfillment of the requirements of degree of Doctor of Philosophy

to the



Indian Institute of Technology Delhi

FEBRUARY, 2026

- I dedicate this thesis to my beloved parents and Lord Venkateswara. My parents have been my first teachers, instilling in me the importance of education, integrity, and perseverance. Their unwavering support and constant encouragement have been my greatest strength throughout this journey. I also offer my deepest gratitude to Lord Venkateswara, whose divine blessings gave me hope and courage during the most challenging moments. This work is a humble offering of my faith, love, and gratitude-

Certificate

This is to certify that the thesis entitled “**Carbon fiber paper electrode of high capacitance for supercapacitor**” submitted by **Peparthi Mythili** to the Indian Institute of Technology Delhi, for the award of the degree of **Doctor of Philosophy** in Chemical Engineering, is a record of bonafide research work carried out by him. Peparthi Mythili has worked under my guidance and supervision and has fulfilled the requirements for the submission of the thesis.

The results contained in this thesis have not been submitted in part or in full to any other university or institute for the award of any degree or diploma.

Anupam Shukla
Department of Chemical Engineering
Indian Institute of Technology, Delhi
India - 110016.

Acknowledgments

I would like to sincerely thank my supervisor, Prof. Anupam Shukla, for his invaluable support, thoughtful insights, and consistent encouragement throughout the course of this research. His mentorship has played an important role in shaping my academic progress and personal development, lessons I will cherish for a lifetime. His intellectual depth, humility, and simplicity continue to inspire me to grow both as a researcher and as a person. Thank you, Sir, for leading me in the right direction and for being a guiding force in this journey.

I would like to express my sincere gratitude to Prof. Anil Kumar Verma, Prof. Gaurav Goel, and Prof. Pravin P. Ingole (Department of Chemistry), for their guidance and constructive feedback throughout my research.

I would like to thank my labmates, Mr. Jayant Nagar, Dr. Rahul Raghuwanshi, Dr. Satirtha Sharma(late), Dr. Pooja Jangir, Dr. Isha Atrey, for their constant support and help during these important years. Their willingness to share knowledge and explain doubts has been useful, especially in the early days of my research. I would like to thank Dr. Lekha Sharma, Dr. Amit Kumar, and Mr. Sachidananda Mohapatra for their kind support and assistance. Their practical help and cooperation were greatly appreciated during a crucial part of my research. I am also grateful to the Central Research Facility for providing access to material

characterization support, which was instrumental in the successful completion of my research.

I would like to express my heartfelt gratitude to my husband, Dr. Sujan Yenuganti for his unwavering support throughout my PhD journey. He stood by me during the most challenging times, offering constant moral support and encouragement at every step. His dedication in taking care of our children while I focused on my research was invaluable. I am forever grateful for his love, patience, and belief in me.

I am profoundly grateful to my beloved parents, Shri Peparthi Narayana Rao and Smt. Peparthi Sarojini, my sister G. Dharani, and my nephew G. Surya for their unwavering emotional support, unconditional love, and countless sacrifices that have shaped me into who I am today and brought me to this stage of life. Finally, I offer my heartfelt thanks to Lord Venkateswara for blessing me with the strength, wisdom, and good health that guided me throughout this journey.

Peparthi Mythili

Abstract

Electric double-layer capacitors (EDLCs), or supercapacitors, have garnered considerable interest in the pursuit of improved energy storage technologies owing to their elevated power density, extended cycle life, and fast charge-discharge capabilities. Nonetheless, a significant constraint that persists in hindering their extensive adoption particularly in portable devices, electric cars, and grid-scale storage is their very low energy density relative to batteries. Confronting this difficulty is essential for closing the performance disparity between batteries and capacitors. Carbon-based materials have been extensively investigated among diverse electrode materials owing to their elevated surface area, electrical conductivity, chemical stability, and economic viability. Carbon fiber paper (CFP) is particularly notable as a viable option due to its high conductivity, mechanical strength, and dual function as both the current collector and active electrode material. Notwithstanding these benefits, clean CFP exhibits low inherent capacitance, hence constraining its efficacy in high-energy-density applications. Consequently, formulating techniques to improve the capacitance and energy density of CFP-based supercapacitors is both urgent and crucial for realizing their full potential in next-generation energy storage systems.

This thesis aims to improve the energy density of carbon fiber paper (CFP)-

based supercapacitors using straightforward and efficient modification techniques. In the initial investigation, CFP underwent anodization in nitric acid, leading to a significant enhancement in specific capacitance by almost three orders of magnitude attributable to the incorporation of oxygen-containing functional groups. In the second study, the anodized CFP was deposited on nickel foam, and mass loading was optimized. This further augmented the electrochemical performance by enhancing conductivity and optimizing active material use. The high-capacitance electrode created in the second investigation was ultimately combined with a water-in-salt NaClO_4 electrolyte. This arrangement markedly enhanced the energy density by expanding the electrochemical stability window.

In the initial study, a self-standing carbon fiber paper (CFP) electrode of high capacitance ($3.96 \text{ F cm}^{-2}/ 198 \text{ F g}^{-1}$) was obtained by increasing the specific capacitance of pristine CFP by three orders of magnitude via a simple, one-step anodization in nitric acid. The FESEM images showed little change in the morphology, but XRD and Raman spectroscopy revealed a substantial increase in structural defects on anodization of the carbon fiber. The different oxygen functionalities introduced on the CFP surface during anodization were determined from the XPS analysis. Electrochemical characterizations, including CV and GCD, were used to measure the capacitance and rate capability of the CFP subjected to different anodization conditions and to determine the contributions of the double layer and pseudocapacitance. As a demonstration, a symmetric supercapacitor fabricated from the electrode displayed excellent specific energy of 14.7 Wh kg^{-1} .

The electrochemical performance of CFP based supercapacitor obtained in the previous study was further improved by synthesizing an electrode from a anodized

carbon fiber paper (CFP) that exhibits a high areal capacitance of 4.42 F cm^{-2} and a specific capacitance of 228 F g^{-1} at a current density of 20 mA cm^{-2} (1 A g^{-1}). The electrode is made by a two-step process that involves the anodization of CFP in nitric acid followed by its deposition onto nickel foam. The impact of mass loading of the anodized CFP on nickel foam has been studied and optimized. A symmetric supercapacitor fabricated with the electrode exhibited an impressive specific energy of 15.6 Wh kg^{-1} .

In the final study, a high energy density aqueous supercapacitor was developed using a high capacitance carbon fiber paper (CFP) based electrode (NiCFP20) and NaClO_4 water-in-salt electrolyte with high electrochemical stable potential window (2.3V). The voltage window of the NiCFP20 electrode in various concentrations of NaClO_4 was evaluated using cyclic voltammetry and further validated through chronoamperometry and electrochemical impedance spectroscopy measurements. The cyclic voltammograms, GCD curves, and EIS spectra reveal the robust electrochemical kinetics of the NiCFP20 electrode in a highly concentrated NaClO_4 water-in-salt electrolyte. The NiCF20 electrode exhibited a high areal capacitance of 3.43 F cm^{-2} (178 F g^{-1}) at 20 mA cm^{-2} (1 A g^{-1}). Further, a symmetric supercapacitor made from electrodes demonstrated exceptional specific energy of 34.75 Wh kg^{-1} at 359.4 W kg^{-1} , and maintained a specific energy of 16 Wh kg^{-1} at 2.6 kW kg^{-1} .

Keywords: Carbon fiber paper, supercapacitor, anodization, nickel foam, water-in-salt electrolyte, energy density, EDLC

Abstract in Hindi

विद्युत द्वि-परत संधारित्रों (ईडीएलसी), या सुपरकैपेसिटर, ने अपने उच्च ऊर्जा घनत्व, विस्तारित चक्र जीवन और तीव्र आवेश-निर्वहन क्षमताओं के कारण, बेहतर ऊर्जा भंडारण तकनीकों की खोज में काफ़ी रुचि अर्जित की है। फिर भी, विशेष रूप से पोर्टेबल उपकरणों, इलेक्ट्रिक कारों और ग्रिड-स्केल भंडारण में, इनके व्यापक रूप से अपनाए जाने में एक महत्वपूर्ण बाधा बैटरियों की तुलना में इनका बहुत कम ऊर्जा घनत्व है। बैटरियों और संधारित्रों के बीच प्रदर्शन असमानता को कम करने के लिए इस कठिनाई का समाधान आवश्यक है। कार्बन-आधारित पदार्थों का उनके उच्च पृष्ठीय क्षेत्रफल, विद्युत चालकता, रासायनिक स्थिरता और आर्थिक व्यवहार्यता के कारण विभिन्न इलेक्ट्रोड पदार्थों में व्यापक रूप से अध्ययन किया गया है। कार्बन फाइबर पेपर (सीएफपी) अपनी उच्च चालकता, यांत्रिक शक्ति और धारा संग्राहक तथा सक्रिय इलेक्ट्रोड पदार्थ, दोनों के रूप में दोहरे कार्य के कारण एक व्यवहार्य विकल्प के रूप में विशेष रूप से उल्लेखनीय है। इन लाभों के बावजूद, स्वच्छ सीएफपी में कम अंतर्निहित धारिता होती है, जिससे उच्च-ऊर्जा-घनत्व वाले अनुप्रयोगों में इसकी प्रभावशीलता सीमित हो जाती है। परिणामस्वरूप, अगली पीढ़ी की ऊर्जा भंडारण प्रणालियों में उनकी पूर्ण क्षमता को साकार करने के लिए सीएफपी-आधारित ईडीएलसी की धारिता और ऊर्जा घनत्व में सुधार करने के लिए तकनीकों का निर्माण करना अत्यावश्यक और महत्वपूर्ण दोनों हैं।

इस शोध प्रबंध का उद्देश्य सरल और कुशल संशोधन तकनीकों का उपयोग करके कार्बन फाइबर पेपर (सीएफपी)-आधारित सुपरकैपेसिटर के ऊर्जा घनत्व में सुधार करना है। प्रारंभिक अध्ययन में, सीएफपी को नाइट्रिक अम्ल में एनोडाइज़ किया गया, जिससे ऑक्सीजन युक्त क्रियात्मक समूहों के समावेश के कारण विशिष्ट धारिता में लगभग तीन क्रम परिमाण की उल्लेखनीय वृद्धि हुई। दूसरे अध्ययन में, एनोडाइज़्ड सीएफपी को निकल फोम पर निक्षेपित किया गया और द्रव्यमान भार को अनुकूलित किया गया। इससे चालकता में वृद्धि और सक्रिय पदार्थ के उपयोग को अनुकूलित करके विद्युत-रासायनिक प्रदर्शन में और वृद्धि हुई। दूसरे अध्ययन में निर्मित

उच्च-धारिता वाले इलेक्ट्रोड को अंततः जल-में-नमक NaClO_4 इलेक्ट्रोलाइट के साथ संयोजित किया गया। इस व्यवस्था ने विद्युत-रासायनिक स्थिरता खिड़की का विस्तार करके ऊर्जा घनत्व को उल्लेखनीय रूप से बढ़ाया।

प्रारंभिक अध्ययन में, नाइट्रिक एसिड में एक सरल, एक-चरण एनोडाइजेशन के माध्यम से तीन क्रम के परिमाण द्वारा प्राचीन सीएफपी की विशिष्ट धारिता को बढ़ाकर उच्च धारिता ($3.96 \text{ F cm}^{-2}/198 \text{ F g}^{-1}$) वाला एक स्व-स्थायी कार्बन फाइबर पेपर (CFP) इलेक्ट्रोड प्राप्त किया गया था। FESEM छवियों ने आकृति विज्ञान में थोड़ा परिवर्तन दिखाया, लेकिन XRD और रमन स्पेक्ट्रोस्कोपी ने कार्बन फाइबर के एनोडाइजेशन पर संरचनात्मक दोषों में पर्याप्त वृद्धि का खुलासा किया। एनोडाइजेशन के दौरान CFP सतह पर पेश की गई विभिन्न ऑक्सीजन कार्यात्मकताओं को XPS विश्लेषण से निर्धारित किया गया था। CV और GCD सहित विद्युत रासायनिक लक्षण वर्णन का उपयोग विभिन्न एनोडाइजेशन स्थितियों के अधीन CFP की धारिता और दर क्षमता को मापने और दोहरी परत और छद्म धारिता के योगदान को निर्धारित करने के लिए किया गया था।

पिछले अध्ययन में प्राप्त सीएफपी आधारित सुपरकैपेसिटर के विद्युत-रासायनिक प्रदर्शन को एनोडाइज्ड कार्बन फाइबर पेपर (सीएफपी) से एक इलेक्ट्रोड के संश्लेषण द्वारा और बेहतर बनाया गया था, जो 20 mA cm^{-2} (1 A g^{-1}) के धारा घनत्व पर 4.42 F cm^{-2} की उच्च क्षेत्रीय धारिता और 228 F g^{-1} की विशिष्ट धारिता प्रदर्शित करता है। यह इलेक्ट्रोड दो-चरणीय प्रक्रिया द्वारा निर्मित होता है जिसमें नाइट्रिक अम्ल में सीएफपी का एनोडाइजेशन और उसके बाद निकल फोम पर उसका निक्षेपण शामिल है। एनोडाइज्ड सीएफपी के द्रव्यमान भार का निकल फोम पर प्रभाव का अध्ययन और अनुकूलन किया गया है। इस इलेक्ट्रोड से निर्मित एक सममित सुपरकैपेसिटर ने 15.6 Wh kg^{-1} की प्रभावशाली विशिष्ट ऊर्जा प्रदर्शित की।

अंतिम अध्ययन में, एक उच्च ऊर्जा घनत्व वाला जलीय सुपरकैपेसिटर विकसित किया गया, जिसमें उच्च धारिता वाले कार्बन फाइबर पेपर (CFP) आधारित इलेक्ट्रोड (NiCFP20) और NaClO_4 जल-में-लवण

इलेक्ट्रोलाइट का उपयोग किया गया, जिसमें उच्च विद्युत-रासायनिक स्थिर विभव विंडो (2.3V) थी। NaClO₄ की विभिन्न सांद्रताओं में NiCFP20 इलेक्ट्रोड की वोल्टेज विंडो का मूल्यांकन चक्रीय वोल्टमेट्री का उपयोग करके किया गया और क्रोनोएम्परोमेट्री तथा विद्युत-रासायनिक प्रतिबाधा स्पेक्ट्रोस्कोपी मापों के माध्यम से आगे इसकी पुष्टि की गई। चक्रीय वोल्टमैमोग्राम, GCD वक्र और EIS स्पेक्ट्रा, अत्यधिक सांद्रित NaClO₄ जल-में-लवण इलेक्ट्रोलाइट में NiCFP20 इलेक्ट्रोड की सुदृढ़ विद्युत-रासायनिक गतिकी को प्रकट करते हैं। NiCF20 इलेक्ट्रोड ने 20 mA cm⁻² (1 A g⁻¹) पर 3.43 F cm⁻² (178 F g⁻¹) की उच्च क्षेत्रीय धारिता प्रदर्शित की। इसके अलावा, इलेक्ट्रोड से बने एक सममित सुपरकैपेसिटर ने 359.4 W kg⁻¹ पर 34.75 Wh kg⁻¹ की असाधारण विशिष्ट ऊर्जा का प्रदर्शन किया, और 2.6 kW kg⁻¹ पर 16 Wh kg⁻¹ की विशिष्ट ऊर्जा बनाए रखी।

मुख्य शब्द: कार्बन फाइबर पेपर, सुपरकैपेसिटर, एनोडाइजेशन, निकेल फोम, जल-इन-सॉल्ट इलेक्ट्रोलाइट, ऊर्जा घनत्व, ईडीएलसी

Contents

Certificate	i
Acknowledgement	iii
Abstract	v
1 Introduction	1
1.1 Electrochemical Energy storage	1
1.2 Capacitors and Supercapacitors	4
1.2.1 Electric Double Layer Capacitors(EDLC)	6
1.2.2 Pseudo-capacitors	8
1.2.3 Hybrid capacitors	10
1.3 Carbon-based electric double layer capacitors	12
1.4 Factors affecting carbon electrode performance	13
1.5 Carbon EDLCs: Challenges and Prospects	19
1.6 Research objectives	22
1.7 Thesis Organization	23
2 Literature review	25
2.1 Materials for Carbon-Based EDLCs: Electrodes and Electrolytes . .	27
2.1.1 Carbon-based electrode materials for EDLC	27
2.1.2 Carbon Synthesis Techniques for EDLCs	38
2.1.3 Electrolytes	46
2.1.3.1 Aqueous electrolytes	46
2.1.3.2 Water in Salt electrolytes	47
2.1.3.3 Organic electrolytes	51

3	Self-standing CFP electrode	53
3.1	Introduction	54
3.2	Experimental	54
3.2.1	Electrode preparation	54
3.2.2	Morphological, structural, and chemical characterizations . .	56
3.2.3	Electrochemical measurements	57
3.2.4	Assembly of symmetric supercapacitors	59
3.3	Results and discussions	59
3.3.1	Structural Characterizations	59
3.3.2	Electrochemical Characterizations	67
3.4	Summary	76
4	Anodized CFP on Ni-foam current collector	79
4.1	Introduction	79
4.2	Experimental section	80
4.2.1	Electrode preparation	80
4.2.2	Electrochemical measurements	81
4.2.3	Assembly of symmetric supercapacitors	82
4.3	Results and Discussion	82
4.3.1	Electrochemical Characterizations	82
4.4	Summary	94
5	Anodized CFP–Ni Foam Electrode in WiSE	95
5.1	Introduction	96
5.2	Experimental section	96
5.2.1	Materials and electrodes	96
5.2.2	Electrochemical measurements	97
5.2.3	Assembly of symmetric supercapacitors	97
5.3	Results and Discussion	98
5.3.1	Electrochemical Characterizations	98
5.3.2	Summary	105
6	Conclusions	107
A	Appendix A	111
A.1	111
References		121

CONTENTS

Publications from the Thesis	151
Author's Biography	154

List of Figures

1.1	Electric Double Layer theory proposed by (a) Helmholtz (b) Gouy-Chapman (c) Gouy-Chapman-Stern	7
1.2	Comparison of charge storage in EDLC,PC, and Battery [1]	9
3.1	A schematic illustration of the electrode synthesis.	55
3.2	FESEM images of (a) pristine CFP, (b)CFP4M,(c) CFP7M,(d) CFP10M,(e) CFP15.7M, (f) & (g) magnified view of a carbon fiber of CFP10M electrode.	61
3.3	TEM micrographs and corresponding SAED patterns of (a, b) pristine CFP and (c, d) CFP anodized in 10 M HNO ₃ (CFP10M).	62
3.4	XRD spectra of CFP electrodes anodized under varying nitric acid concentrations.	63
3.5	(a) Raman spectra, (b) detailed view of the D and G regions with separation of the G band into G and D' components,(c) variation in the I_D/I_G ratio, and (d)(I_D/I_G) vs ($I_{D'}/I_G$) plot for CFP electrodes.	64
3.6	The XPS (a) survey spectra for the CFP electrodes, and (b) high-resolution C _{1s} peak along with its deconvoluted components for the CFP10M electrode.	65
3.7	Cyclic voltammograms (4th cycle, at 10 mV s ⁻¹) for the CFP electrodes (a) anodized at different current densities in 5 M nitric acid, as well as (b) cyclic voltammograms (at 10 mV s ⁻¹), (c) GCD curves (4 th) cycle at 5 mA cm ⁻²), (d) the EDLC and pseudocapacitive components, and (e) Nyquist plot for the CFP electrodes anodized at 150 mA cm ⁻² in nitric acid of different concentrations. For pristine CFP, the GCD curve in part (c) was taken at 0.1 mA cm ⁻²	69
3.8	(a) GCD profiles (4 th cycle) (b) areal capacitance of CFP10M electrode at different current densities and (c) Cyclic stability of CFP10M electrode at 100 mA cm ⁻²	72

LIST OF FIGURES

3.9	(a) A comparison of the symmetric capacitor of this work with the values reported in recent literature for carbon based EDLC on a Ragone plot, (b)cyclic stability of AQSSC at 40 mA cm ⁻² (c)cyclic stability of ORSSC at 40 mA cm ⁻² (d) two AQSSC lighting a LED, and (e) one ORSSC lighting a LED	75
4.1	A schematic illustration of the electrode synthesis process.	81
4.2	Comparison of electrochemical characteristics of NiCFP10, NiCFP15, NiCFP20, and NiCFP25 electrodes: (a) Cyclic voltammetry (CV) curves, (b) galvanostatic charge–discharge (GCD) curves, (c) specific capacitance as a function of mass loading, and (d) Nyquist plots derived from electrochemical impedance spectroscopy (EIS).	83
4.3	Integrated charge(q) at different potential steps vs t ^{1/2} for (a) NiCFP10, (b) NiCFP15, (c) NiCFP20, and (d) NiCFP25 electrodes	86
4.4	Intercepts of q vs t ^{1/2} regression lines of Figure 4.3 plotted against the corresponding potential steps for (a) NiCFP10, (b) NiCFP15, (c) NiCFP20, and (d) NiCFP25 electrodes	87
4.5	EDLC and PC contribution of NiCFPX electrodes with different mass loadings	88
4.6	(a) Comparison of GCD curves for NiCFP20 and CFP10M (b) Comparison of Nyquist plots for NiCFP20 and CFP10M (c) GCD curves at different charge-discharge current densities (d) Specific capacitance at different discharge current densities	89
4.7	Performance of AQSSC(a) CV curves at different scan rates (b) GCD curves at different discharge current densities (c) Nyquist plot. Performance of ORSSC (d)CV curves at different scan rates (e) GCD curves at different discharge current densities (f) Nyquist plot	92
4.8	Cyclic stability and coulombic efficiency for(a) AQSSC (b) ORSSC (c) A comparison of the symmetric supercapacitors from this study with the values documented in the literature for carbon-based supercapacitors on a Ragone plot	93
4.9	(a) Two AQSSC lighting an LED, and (b) one ORSSC lighting an LED	94
5.1	Potential window determination using CV curves (a) 1m NaClO ₄ (b)9m NaClO ₄ (c) 11m NaClO ₄	99

LIST OF FIGURES

5.2	Chronoamperograms (a) Positive voltage range; (b) negative voltage range; EIS curves in (c) positive voltage range and (d) negative voltage range.	100
5.3	(a)CV curves (b) GCD profiles and (c) Nyquist plot of NiCFP20 electrode in water-in-salt electrolyte.	102
5.4	Performance of Symmetric supercapacitor assembled with NiCFP20 and 11m NaClO ₄ electrolyte (a)CV curves at different scan rates(b) GCD profiles at various current densities (c) Nyquist plot	104
A.1	Current-potential profile of the anodization process in three electrode setup. The curve is for the CFP electrode anodized at 0.15A for 800s	112
A.2	EDX Elemental mapping of (a) PCFP electrode (b) CFP10M electrode	113
A.3	(a)Magnified view of 004 diffraction peak (b) Enlarged section highlighting the 006 diffraction reflection	113
A.4	XPS high resolution C _{1s} peak with deconvoluted component peaks for (a) CFP1M, (b) CFP4M, (c) CFP7M, and (d) CFP15.7M . . .	114
A.5	BET isotherms for pristine CFP(PCFP), CFP4M, CFP7M, CFP10M, CFP15.7M electrodes	115
A.6	Current–voltage characteristics obtained through four-point probe measurements of pristine and anodized CFP electrodes	115
A.7	Integrated charge (q) at different potential steps vs t _{1/2} for (a) CFP4M, (b) CFP7M, (c) CFP10M, and (d)) CFP15.7M electrodes	116
A.8	: Intercepts of q vs t _{1/2} regression lines of Figure A7 plotted against the corresponding potential steps for (a) CFP4M, (b)) CFP7M, (c) CFP10M, and (d)) CFP15.7M electrodes	117
A.9	Performance of AQSSC(a) CV curves (b) GCD curves (e) Nyquist plot. Performance of ORSSC (c) CV curves (d) GCD curves(f)Nyquist plot	118
A.10	IR drop vs. current densities for AQSSC and ORSSC	119
A.11	CV response of bare Ni foam recorded in 6M KOH	119
A.12	Electrochemical stability window optimization (2.3 V) in 11 m NaClO ₄ via CV and CA analysis	120

List of Tables

1.1	A comparison of the electrochemical properties of a capacitor, a supercapacitor and a battery. Data taken from [2].	3
2.1	Performance of Carbon-Based EDLC	45
3.1	The surface elemental composition of CFP electrodes determined from XPS.	66
3.2	A comparison of the capacitance of carbon fiber paper/carbon fiber based supercapacitor electrodes	74
4.1	The best-fit parameters of the equivalent circuit model used to simulate the impedance spectra of the NiCFPX electrodes	84
4.2	A comparison of the capacitance of carbon based electrodes for supercapacitor	91
A.1	The surface composition of anodized electrodes, corresponding to the functional groups C=C, C-C, C-OH, C-O-C, C=O, and COOH, was quantified from the integrated areas of deconvoluted C1s spectral components illustrated in Figure S2.	111
A.2	Total pore volume and micropore volume obtained from the Horvath-Kawazoe (HK) plot for pristine and anodized electrodes.	111
A.3	Electrical resistance of CFP electrodes as determined through four-point probe measurements	112
A.4	The best-fit parameters of the equivalent circuit model used to simulate the impedance spectra of the anodised CFP electrodes R_1 (Ω)-solution resistance, C_1 (F)-double layer capacitance, R_2 (Ω)-ohmic resistance, Y_{o1} ($S s^a$), A-constant phase element and Y_{o2} ($S s^{0.5}$), B_1 ($s^{0.5}$)- a Warburg component.	112

Nomenclature and list of abbreviations

Symbol	Definition
q	charge stored on the plates
d	distance between charged plates
ϵ_o	Permittivity of free space ($F\ m^{-1}$)
ϵ	Relative permittivity of dielectric ($F\ m^{-1}$)
C	Capacitance
E	Energy density
P	Power density
t	time of discharge
R_{ESR}	Equivalent series resistance
C_{DL}	Total double layer capacitance
C_{Stern}	Capacitance of stern layer
$C_{Diffuse}$	Capacitance of diffuse layer
C_A	areal capacitance
C_m	specific capacitance
λ	Wavelength (nm)
θ	Angle of diffraction ($^\circ$)
R	Universal gas constant ($J\ mol^{-1}\ K^{-1}$)
K	Rate constant
v/v	Volume/volume
Z_{im}	imaginary component of impedance (Ω or $\Omega\ cm^2$)
T	Temperature ($^\circ C$ or K)
f	Applied frequency (Hz)

j	Current density (A cm^{-2})
$ Z $ (Ω or $\Omega \text{ cm}^2$)	Absolute value of impedance
V	Voltage (V)
F	Faraday constant (C mol^{-1})
I	Current (A)
Z_{re}	real component of impedance (Ω or $\Omega \text{ cm}^2$)
A	Area of electrode (cm^2)
ν	Scan rate (V/s)
ΔV	Voltage window (V)
R_{CT}	Charge transfer resistance ($\Omega \text{ cm}^2$)
D	diffusion coefficient
C	surface concentration
R_S	Solution resistance ($\Omega \text{ cm}^2$)
Z_W	Warburg impedance ($\text{s}^{0.5} \Omega^{-1} \text{ cm}^{-2}$)
ω	angular frequency (rad/s)
I_D	Intensity of D peak
I_G	Intensity of G peak
$I_{D'}$	Intensity of D peak
C_{1s}	Carbon 1s orbital

Abbreviation

Description

Na	Sodium
N_2	Nitrogen
Pt	Platinum
Ni	Nickel
Ag	Silver
Hg	Mercury
CFP	Carbon fiber paper
NMP	N-Methyl-2-pyrrolidone
IHP	Inner Helmholtz plane
OHP	Outer Helmholtz plane
CB	carbon black
CNT	Carbon nanotubes
CDC	Carbon derived carbon

ESPW	electrochemical stable potential window EDLC
Electric double layer capacitor	
PC	Pseudocapacitance
SC	Supercapacitor
EC	Electrochemical capacitor
HNO ₃	Nitric acid
H ₂ SO ₄	Sulfuric acid
NaNO ₃	Sodium nitrate
KOAc	Potassium acetate
AgCl	Silver chloride
HgO	mercuric oxide
CH ₃ COOK	potassium acetate
PVDF	Polyvinylidene Fluoride
TEABF ₄	Tetraethylammonium tetrafluoroborate
NaClO ₄	Sodium perchlorate
WiSE	Water-in-salt electrolyte
XRD	X-ray diffraction
SAED	Selected area electron diffraction
FESEM	Field emission scanning electron microscopy
TEM	Transmission electron microscope
EDX	Energy dispersive X-ray
XPS	X-ray photoelectron spectroscopy
SSC	symmetric supercapacitors
AQSSC	Aqueous symmetric supercapacitor
ORSSC	Organic symmetric supercapacitor
CV	Cyclic voltammetry or cyclic voltammogram
BET	Brunauer-Emmett-Teller
3D	Three-dimensional
DC	Direct current
EIS	Electrochemical impedance spectroscopy
CPE	Constant phase element
AC	Alternating current
PCFP	Pristine CFP
CFP4M	CFP electrodes anodized in 4M HNO ₃
CFP7M	CFP electrodes anodized in 7M HNO ₃
CFP10M	CFP electrodes anodized in 10M HNO ₃
CFP15.7M	CFP electrodes anodized in 15.7M HNO ₃

FWHM	full width at half maximum
LED	Light emitting diode
NiCFP10	CFP10M(10 mg cm ⁻²) loaded on Nickel foam
NiCFP15	CFP10M(15 mg cm ⁻²) loaded on Nickel foam
NiCFP20	CFP10M(20 mg cm ⁻²) loaded on Nickel foam
NiCFP25	CFP10M(25 mg cm ⁻²) loaded on Nickel foam